Monte Carlo simulation study of quasi-elastic electron scattering from an overlayer/substrate system

2008 J. Phys.: Condens. Matter 20 355005

(http://iopscience.iop.org/0953-8984/20/35/355005)

J. Phys.: Condens. Matter **20** (2008) 355005 (9pp) doi:10.1088/0953-8984/20/35/355005

Monte Carlo simulation study of quasi-elastic electron scattering from an overlayer/substrate system

Y G Li[1], Z M Zhang[2], S F Mao[1] and Z J Ding[1]

[1] Hefei National Laboratory for Physical Sciences at the Microscale and Department of Physics, University of Science and Technology of China, Hefei, Anhui 230026, People's Republic of China
[2] Department of Astronomy and Applied Physics, University of Science and Technology of China, Hefei, Anhui 230026, People's Republic of China

E-mail: zjding@ustc.edu.cn

Received 10 May 2008, in final form 13 July 2008
Published 1 August 2008
Online at stacks.iop.org/JPhysCM/20/355005

Abstract

Recent experimental results have shown that the recoil energies of electrons elastically scattered by light and heavy atoms can be resolved for an energetic electron beam and at large scattering angles. Full understanding of the scattering processes involved is helpful to sample characterization, and for providing more knowledge about electron inelastic mean free path. In this work we use a Monte Carlo simulation method to quantitatively study the energy shift, the Doppler broadening and, especially, the peak intensity ratio for an overlayer/substrate sample. Recoil energy in the electron elastic scattering events is calculated on the basis of our previous Monte Carlo simulation model by taking account of the kinetic energy of atoms. An anisotropic distribution of the velocity direction of the atoms, the Maxwell–Boltzmann thermal energy distribution and also the multiple scattering of electrons are considered in the simulation. By introducing a polarized momentum a good agreement has been obtained on the position shift of the quasi-elastic peak between the calculation and experiment. The calculation also shows a quantitative agreement with the experimental results on the peak intensity ratio between different elements for a Ge/C overlayer sample. It is illustrated that the multiple-scattering effect is remarkable for a high energy beam.

1. Introduction

Electron elastic scattering at surfaces provides an effective way of determining the physical parameters related to electron transport processes, such as electron inelastic mean free path (IMFP), by elastic peak electron spectroscopy (EPES) [1]. The recoil effect in quasi-elastic scattering of electrons was first described by Boersch *et al* as early as 1967 [2]. It was shown that there is an energy loss involved in large-angle elastic scattering events, consistent with momentum transfer to a single atom in the scattering event. The quasi-elastic peak is a marked feature in EPES spectra. From then on, the recoil effect of the elastic peak in electron spectroscopy has been paid much attention. A lot of experimental works have been performed to study the energy shift and broadening of the quasi-elastic peak spectra for the elemental solids [3–5], organic polymer solids [6–8], compounds [9] and overlayer systems [10–13] by varying the atomic number of the sample. Recently it has been shown that, by using an energetic electron beam (20–40 keV) and at large scattering angles, the recoil energies for atoms with large mass difference can be resolved [9–13]. The technique is termed electron Rutherford backscattering (ERBS) [9].

On the other hand, Monte Carlo simulations of the energy shift and recoil broadening of the elastic peak in electron spectra were performed later for similar systems by using classical approaches [14, 15]. Also, a quantum scattering theory including the recoil effect has been proposed for dealing with elastically scattered electrons and photoelectrons involved in electron spectra [16]. However, these works have not yet derived the intensity ratio between peaks that are attributed to different elements, and only one simple analysis of the intensity ratio was given, in [12]. Accurate description of the

peak intensity ratio as well as peak shape provides important information on electron scattering processes involved and related physical mechanisms, which will certainly be helpful for providing more knowledge about the electron IMFP and sample characterization—such as for unique determination of the thickness of an overlayer, in-depth distribution of elements and composition.

In this paper, we use a Monte Carlo simulation method to quantitatively study the energy shift, the Doppler broadening and, especially, the peak intensity ratio for an overlayer/substrate system. The simulation is chiefly based on our previous Monte Carlo model of electron scattering [17–19], but also considering the Maxwell–Boltzmann thermal energy distribution of atoms with an anisotropic distribution of the velocity direction by introducing a polarized momentum component. For comparison with experimental observation, the simulation of quasi-elastic scattering of electrons of energies about 15–30 keV from a Ge/C overlayer either in reflection geometry or transmission geometry has been performed. The simulated peak intensity ratio agrees very well with the experimental data. The anisotropic velocity distribution has successfully described the position of the energy shift of the elastic peak.

2. Theory

2.1. Recoil energy

The classical model of the electron quasi-elastic scattering from a free atom is used for its simplicity and validity in most cases [14, 15]. Went and Vos [20] have considered in detail why the electron quasi-elastic scattering can certainly be described as scattering by a free atom, while the fact that the atom is part of a crystal is assumed not to influence the result. Thus, it is convenient and reasonable to use the binary encounter approximation instead of the electron–lattice interaction for the electron quasi-elastic scattering, for the impulse approximation is valid here. If an incoming electron of mass m with momentum $\mathbf{P}$ is elastically scattered over an angle θ by an atom of mass M, the momentum change is approximately about $q \simeq 2P\sin(\theta/2)$. Assuming that the target atom is at rest initially before the collision; the energy transferred from an electron to an atom is

$$E_{\mathrm{r0}} = \frac{2mE[(M + m\sin^2\theta) - \sqrt{M^2 - m^2\sin^2\theta}\cos\theta]}{(M+m)^2}, \tag{1}$$

where $E = P^2/2m$ denotes the kinetic energy of the electron. As $m \ll M$, the recoil energy of the electron is approximated as

$$E_{\mathrm{r0}} \simeq q^2/2M = \frac{4m}{M}E\sin^2(\theta/2). \tag{2}$$

More realistically, the target atoms have a kinetic energy due to thermal motion. The recoil energy is then given by the following relation:

$$E_{\mathrm{r}} = \frac{(\mathbf{q}+\mathbf{k})^2}{2M} - \frac{k^2}{2M} = \frac{q^2}{2M} + \frac{\mathbf{q}\cdot\mathbf{k}}{M}, \tag{3}$$

where $\mathbf{k}$ is the initial momentum of the target atoms. The momentum $\mathbf{k}$ here is usually considered as isotropically distributed. The first term in the above equation represents the energy shift of the elastic peak and the second one is the Doppler broadening term due to the vibration of the target atoms in different directions. The classical thermal vibration model has been used to describe the motion of atoms in a solid by considering that the atoms will behave like a classical gas and will have an average kinetic energy $3kT/2$ in the present high temperature case. Only in the low temperature limit should quantum physics be employed to relate Doppler broadening to the interaction of electrons with phonon modes of a lattice.

It has been shown that the recoil energy calculated by using the above classical approach could not yield a good agreement with the experimental value, and a deviation of the peak position was found in comparison [14, 15, 21]. For the cause of such deviation Kwei *et al* [15] considered that the recoil energy should be centered at the most probable value of this loss for vibrating atoms rather than for atoms at rest. However, even taking into account the thermal motion of atoms the simulation overestimates recoil energy when compared with experiments [14]. The reason is quite obvious: the statistical averaging of the second term in equation (3) for isotropic vibrating atoms gives vanishing contribution to the recoil energy and, thus, the simple treatment using equation (3) yields the same peak position as for rest atoms except that the peak is broadened. Vos and Went [21] suggested that the classical thermal distribution cannot describe experiment, considering the differences in peak position and shapes between experimental and expected results. In order to solve this problem, an improved scheme is introduced in this paper. The main idea is to consider that the thermal vibration of target atoms may no longer be regarded as isotropically distributed, for the Coulomb interaction between an energetic incident electron and the target atom can influence the atomic motion through the polarization of atomic electron clouds.

Hence, a proper approach to the description of the anisotropic vibration of the target atoms should be necessary. We assume in the classical approximation that the anisotropic vibration may be described by an elliptical distribution and, accordingly, the momentum vector of atomic motion is composed of an isotropic momentum $\mathbf{k}$ and a preferential oriented momentum $\mathbf{k}_0$. In order to estimate the value and the direction of the momentum component $\mathbf{k}_0$ at least for qualitative analysis, we now analyze the difference between the real momentum change $\mathbf{q}'$ in an experiment and the ideal momentum change $\mathbf{q}$ for a binary collision in a classical theory. The experimental fact indicates $q' < q$ which we attribute to the effect of atomic polarization during collision between charged particles. This is because the electron–atom scattering dynamics accompanies the change of electrostatic potential of an electron, with the induced polarization of atomic electron clouds. These two factors then drive the motion of the atomic nucleus. As the polarization is a directional effect, it is quite reasonable to treat the thermal vibration of target atoms as anisotropically distributed, but not as a simple isotropic distribution for a collision between

hard spheres. Then we can decompose the momentum of the nucleus into two components, an isotropic momentum $\mathbf{k}$ and a preferentially oriented momentum $\mathbf{k}_0$. This simple phenomenological treatment averages the overall polarization effect for an amount of scattering events into a single term within the framework of a classical binary collision theory.

The recoil energy is thus now rewritten as

$$E_r = \frac{(\mathbf{q}+\mathbf{k}+\mathbf{k_0})^2}{2M} - \frac{(\mathbf{k}+\mathbf{k_0})^2}{2M} = \frac{q^2}{2M} + \frac{\mathbf{q}\cdot\mathbf{k}}{M} + \frac{\mathbf{q}\cdot\mathbf{k_0}}{M}, \tag{4}$$

where $(\mathbf{q}+\mathbf{k}+\mathbf{k_0})^2/2M$ and $(\mathbf{k}+\mathbf{k_0})^2/2M$ are the kinetic energies of the atoms before and after the collision. The momentum conservation and energy conservation are valid in such an expression. In addition to the two terms in equation (3), which describe the energy shift and the Doppler broadening of the elastic peak, the third term in the above equation treats the negative shifting of the peak position as due to the anisotropic vibration of the target atoms.

For we can also write the recoil energy as

$$E_r = \frac{(\mathbf{q}'+\mathbf{k})^2}{2M} - \frac{k^2}{2M}, \tag{5}$$

by keeping the same form as in equation (3) but replacing the ideal $\mathbf{q}$ with the measured $\mathbf{q}'$; $\mathbf{k_0}$ is then given by

$$\mathbf{k_0} = -\frac{\mathbf{q}}{2q^2}[(q^2 - q'^2) + 2(\mathbf{q}-\mathbf{q}')\cdot\mathbf{k}]. \tag{6}$$

Therefore, $\mathbf{k}_0$ is oppositional to $\mathbf{q}$ and its effect is to reduce the value of q. In the bracket of above equation, the first term represents the position shift of the peaks, which has been introduced in the present Monte Carlo simulation model. The second term is a minor Doppler broadening term for the shifting. In our simulation model, we have reasonably neglected this minor and symmetrical broadening term. The peak position shift is thus taken as $k_0 = (q^2 - q'^2)/2q$.

To be more clear, we rewrite equation (4) as follows:

$$E_r \approx \left[1 - \frac{k_0}{P}\frac{1}{\sin(\theta/2)}\right]\frac{q^2}{2M} + \frac{\mathbf{q}\cdot\mathbf{k}}{M}. \tag{7}$$

The first term can thus be reasonably taken as the most probable value of the recoil loss energy for anisotropic vibrating atoms and the second term is for the Doppler broadening. It is shown that the most probable value of the recoil energy loss corresponding to the peak position of the spectra will tend to be smaller than E_{r0}, as indicated by the experimental facts. Here, we have neglected the final state effects in the above discussion for it appears to be only a minor part for the deviation of the elastic peak positions [21].

In our Monte Carlo simulation, it is convenient to use the scalar form for each scattering event along electron trajectories:

$$E_r = \frac{2m}{M}E\left\{\left[1 - \frac{k_0}{P}\frac{1}{\sin(\theta/2)}\right](1-\cos\theta) + \sqrt{\frac{M\varepsilon}{mE}}(\cos\vartheta - \cos\theta\cos\vartheta - \sin\theta\sin\vartheta\cos\varphi)\right\}, \tag{8}$$

where ε is the kinetic energy of the isotropic vibration of the target atoms, whose value follows the Maxwell–Boltzmann thermal energy distribution with the mean kinetic energy $\overline{E}_k = 3kT/2$; ϑ and φ are the polar and azimuthal angles characterizing the velocity direction of an atom related to the moving direction of an incident electron.

2.1.1. Electron elastic scattering. Monte Carlo simulation is based on the tracing of electron trajectories made by the joining of randomly sampled electron scattering events [17, 22]. For the treatment of electron elastic scattering, the Mott cross section [23] with the Thomas–Fermi–Dirac atomic potential [24] is employed:

$$\frac{d\sigma_e}{d\Omega} = |f(\theta)|^2 + |g(\theta)|^2, \tag{9}$$

where the scattering amplitudes

$$f(\theta) = \frac{1}{2ik}\sum_{l=0}^{\infty}\{(l+1)(e^{2i\delta_l^+} - 1) + l(e^{2i\delta_l^-} - 1)\}P_l(\cos\theta);$$
$$g(\theta) = \frac{1}{2ik}\sum_{l=1}^{\infty}\{-e^{2i\delta_l^+} + e^{2i\delta_l^-}\}P_l^1(\cos\theta), \tag{10}$$

are calculated by the partial wave expansion method [25]. In the above equation $P_l(\cos\theta)$ and $P_l^1(\cos\theta)$ are, respectively, the Legendre and the first-order associated Legendre functions; δ_l^+ and δ_l^- are spin-up and spin-down phase shifts of the ℓth partial wave, respectively.

2.2. Electron inelastic scattering

A dielectric function modeling based on Penn's theory [26] yields the Bethe stopping powers at high energies; the calculated electron IMFP fits also the experimental data over a wide energy region from several eV to above several keV for many elements and compounds [27–29]. We employed this dielectric function modeling to treat electron inelastic scattering in the simulation. The double-differential cross section for inelastic scattering of electrons in a solid is represented in dielectric theory in terms of the energy loss function $\mathrm{Im}\{-1/\varepsilon(q,\omega)\}$ as

$$\frac{d^2\lambda_{in}^{-1}}{d(\hbar\omega)\,dq} = \frac{1}{\pi a_0 E}\mathrm{Im}\left\{\frac{-1}{\varepsilon(q,\omega)}\right\}\frac{1}{q}, \tag{11}$$

where a_0 is the Bohr radius, $\hbar\omega$ is the energy loss, $\hbar q$ is the momentum transfer from an electron of kinetic energy E penetrating into a solid of dielectric function $\varepsilon(q,\omega)$ and λ_{in} is the electron IMFP. The energy loss distribution and angular distribution of electron inelastic scattering, which are necessary for a Monte Carlo simulation of electron individual inelastic scattering events, can be obtained from the above expression by assuming a dispersion relation [17, 30].

3. Results and discussion

For comparison with the experimental results [12], the calculation conditions are set the same as in the experiment:

Table 1. List of the parameters used in the simulation.

Element	Density (g cm^{-3})	Thickness (Å)	$\overline{E}_k$ (meV)	k_0 (Å^{-1}) ($\theta = 45°$)
C	2.267	350	108 [31]	4.77
Ge	5.32	2, 20	38.8	5.24

(1) the samples are composed of a 0.2 or 2 nm thick Ge layer on a carbon film 35 nm thick; (2) the incident electron beam energy is 15–30 keV; (3) the electron beam has energy width of 0.23 eV (FWHM), and the energy resolution of an energy analyzer is 0.14 eV; these two values are used for convolutions of a Gaussian distribution with the directly simulated spectra at an ideal resolution of 20 meV; (4) the scattering angle is 45°; the acceptance polar angle range, $\Delta\theta \simeq \pm 1°$, is slightly larger than the experimental one for increasing the calculation efficiency; the azimuthal angle range, $\Delta\varphi = 13°$, is the same as that in the experiment.

For fitting with the experimental spectrum, there are two other parameters included in the simulation: the mean kinetic energy $\overline{E}_k$ and the preferential momentum k_0. They can be obtained by fitting the experimental spectrum; the parameters obtained for C and Ge are given in table 1. The mean kinetic energy of 108 meV for C used here was derived from neutron Compton scattering [31]. The FWHM of Ge peak roughly estimates a value of the mean kinetic energy for Ge atoms with the classical Maxwell–Boltzmann thermal energy distribution, and then the value was further corrected by a Monte Carlo simulation until the calculated FWHM fitted with the experimental results. The momentum k_0 of the nucleus is considered to be correlated with the atomic number and the scattering angle but hardly with the incident electron energy. A unique value of k_0 can be obtained in the incident electron energy range from 10 to 40 keV for a specified element and scattering angle by using equation (6) with a fitting procedure.

Figure 1 shows the simulated electron energy spectra for a 30 keV beam penetrating a 2 nm Ge layer on a 35 nm carbon layer sample without taking into account the energy resolution of the equipment. The upper inset shows clearly that the elastic peak is split into two broadening peaks corresponding to the effects of recoil by Ge and C atoms. The lower inset illustrates the loss spectrum in the energy loss region due to plasmon excitation in each film. The optical energy loss functions used here for glassy carbon [32] and Ge [33] have a strong peak around 20 eV (for Ge, the optical data are absent in the photon energy range of 10–20 eV); for C there is another weaker peak present in the energy loss function at about 5.6 eV due to π-plasmons, which corresponds to the small 6.3 eV peak in the lower inset of figure 1. In figure 2 the experimental spectra are compared with the simulated spectra in the classical model for isotropically vibrating atoms and with the simulated spectra in the present model for anisotropically vibrating atoms with the factor k_0. It is shown that on introducing the preferential momentum k_0 the correct peak position is obtained. In this figure and the following figures all the simulated spectra have been convoluted with Gaussian functions for the electron beam energy width and for the energy resolution of energy analyzer.

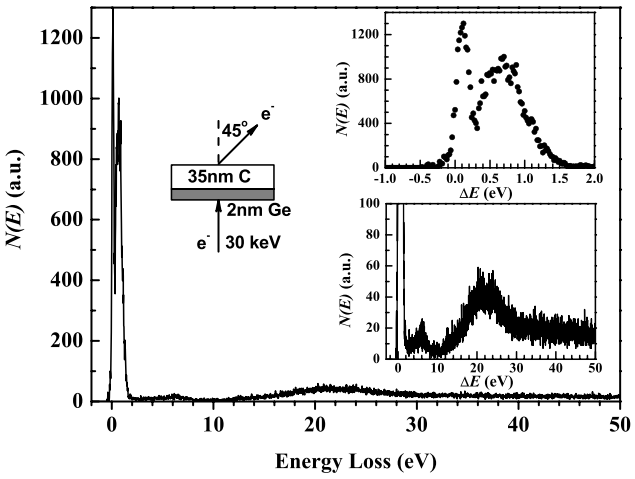

Figure 1. An example of the Monte Carlo simulated transmission $N(E)$ electron spectra for a 30 keV electron beam incident normally on a Ge(2 nm)/C(35 nm) sample at an ideal energy resolution. The inserts show the quasi-elastic peak (top) and the Ge and C plasmon losses in eV (bottom).

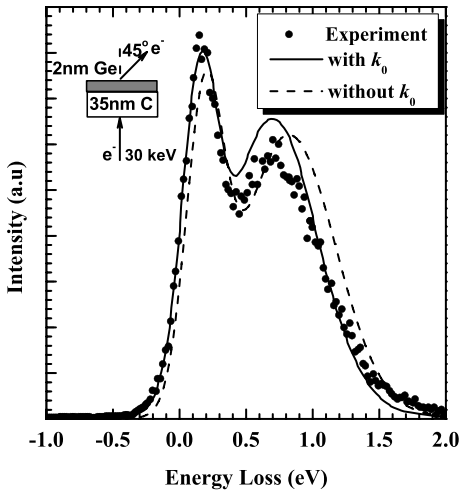

Figure 2. A comparison on the quasi-elastic electron spectra, for a 30 keV electron beam incident normally on a Ge(2 nm)/C(35 nm) sample with Ge layer at the exit side, between the experimental measurement and the Monte Carlo simulations with and without the position shift correction factor k_0.

Figure 3 shows in detail the comparison of the present Monte Carlo simulation results with the experiments at different conditions of film thickness, sample orientation and primary energy. It can be seen that an excellent agreement on the peak position as well as intensity profile has been achieved with the parameters obtained, $\bar{E}_k$ and k_0. As the quasi-elastic peak is now well split into two peaks the Gaussian function fitting to the spectra can give the intensity ratio, A_{Ge}/A_C, between the areas under the respective Gaussian component curves while omitting the residual background. Table 2 presents the detailed comparison on the quantitative values. Clearly, the treatment of the peak shifting is quite reasonable in all the cases considered here.

Figure 4 gives the ratio on the elastic peak intensities between Ge and C, A_{Ge}/A_C, for different thicknesses

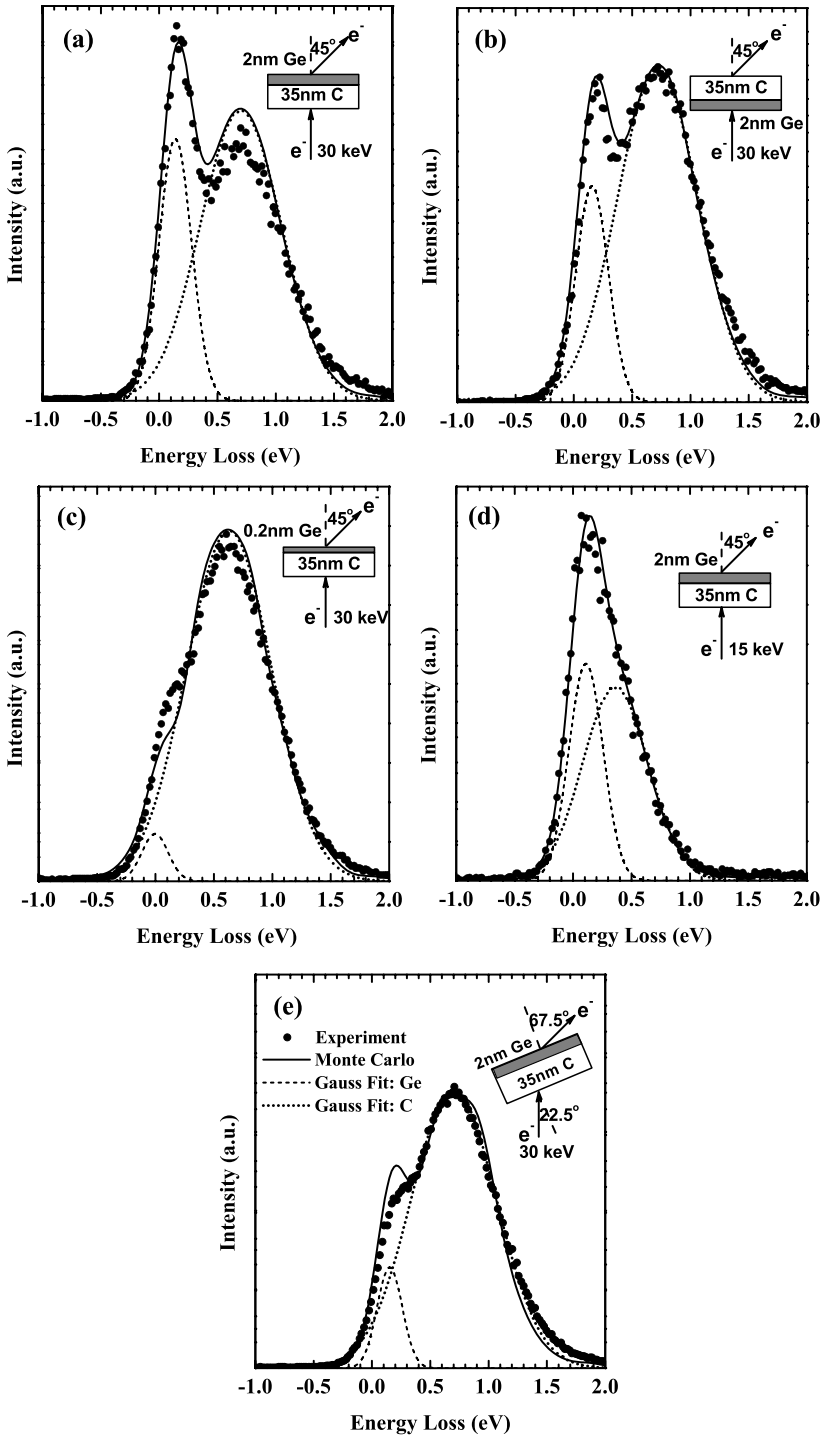

Figure 3. A comparison of the Monte Carlo simulation results of quasi-elastic peak with the experimental measurements for different conditions: (a) $E_0 = 30$ keV, $\theta_{in} = 0°$, $\theta_{out} = 45°$, Ge(2 nm)/C(35 nm) with the Ge layer at the exit side, transmission mode; (b) $E_0 = 30$ keV, $\theta_{in} = 0°$, $\theta_{out} = 45°$, Ge(2 nm)/C(35 nm) with the C layer at the exit side, transmission mode; (c) $E_0 = 30$ keV, $\theta_{in} = 0°$, $\theta_{out} = 45°$, Ge(0.2 nm)/C(35 nm) with the Ge layer at the exit side, transmission mode; (d) $E_0 = 30$ keV, $\theta_{in} = 22.5°$, $\theta_{out} = 67.5°$, Ge(2 nm)/C(35 nm) with the Ge layer at the exit side, transmission mode. E_0 represents the incident energy; θ_{in} and θ_{out} denote, respectively, the incident angle and emission angle of electrons measured from the surface normal.

(0.2–2.0 nm) of a Ge layer on a 35 nm thick carbon layer sample. A good agreement with the experimental data at the two ends of the thickness range has been obtained. An exact linear relation between the ratio and the thickness of the Ge layer is just as expected. This is because the intensity of Ge would be proportional to the distance of electron transmission, or the number of the elastic scattering events is proportional to the thickness of material that electrons pass through in a straight line when a film is not too thick.

We have also studied the energy dependence of the elastic peak profile for the transmission geometry and for a 2 nm Ge on a 35 nm C sample (Ge is at the exit side). Figure 5(a) shows

Table 2. Comparison of various quantities (recoil energy loss, ΔE; full width at half-maximum of the quasi-elastic peak, FWHM; ratio between the peak areas due to Ge and C atoms, A_{Ge}/A_C) between the Monte Carlo simulation (MC) (figure 3), the experiments [12] and simple theoretical analysis [12] by using IMFPs of [28] or [29] for the varied experimental conditions.

(Thickness of Ge film, primary energy, incident angle)	ΔE observed (eV)	ΔE MC (eV)	FWHM Ge observed (eV)	FWHM Ge MC (eV)	FWHM C observed (eV)	FWHM C MC (eV)	Ratio A_{Ge}/A_C observed	Ratio A_{Ge}/A_C MC	Ratio A_{Ge}/A_C theory IMFP [28]	Ratio A_{Ge}/A_C theory IMFP [29]
(2 nm, 30 keV, 0°) Ge at exit side	0.54	0.553	0.29	0.315	0.86	0.833	0.36	0.363	0.73	0.79
(2 nm, 30 keV, 0°) C at exit side	0.54	0.552	0.26	0.318	0.85	0.828	0.17	0.259	0.53	0.48
(0.2 nm, 30 keV, 0°) Ge at exit side	0.54	0.548	0.22	0.227	0.85	0.769	0.044	0.042	0.07	0.08
(2 nm, 15 keV, 0°) Ge at exit side	0.25	0.254	0.31	0.342	0.59	0.621	0.51	0.580	—	—
(2 nm, 30 keV, 22.5°) C at exit side	0.53	0.519	0.25	0.227	0.84	0.817	0.09	0.106	0.33	0.23

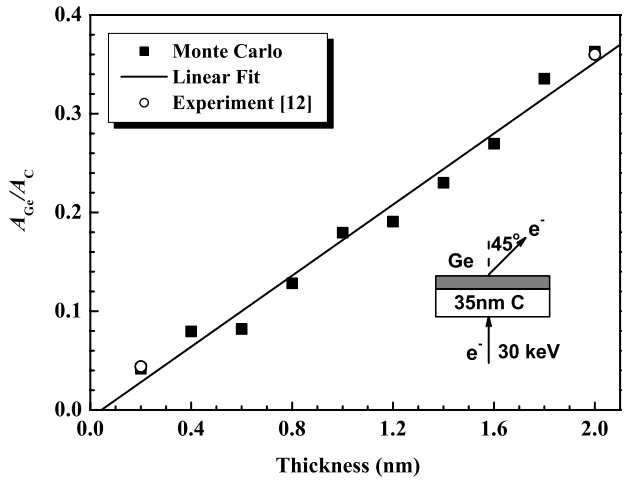

Figure 4. The dependence of the elastic peak intensity ratio, A_{Ge}/A_C, on the thickness of a Ge layer deposited on a C layer of 35 nm thick with the Ge layer on the exit side in the transmission mode for a normally incident electrons of 30 keV.

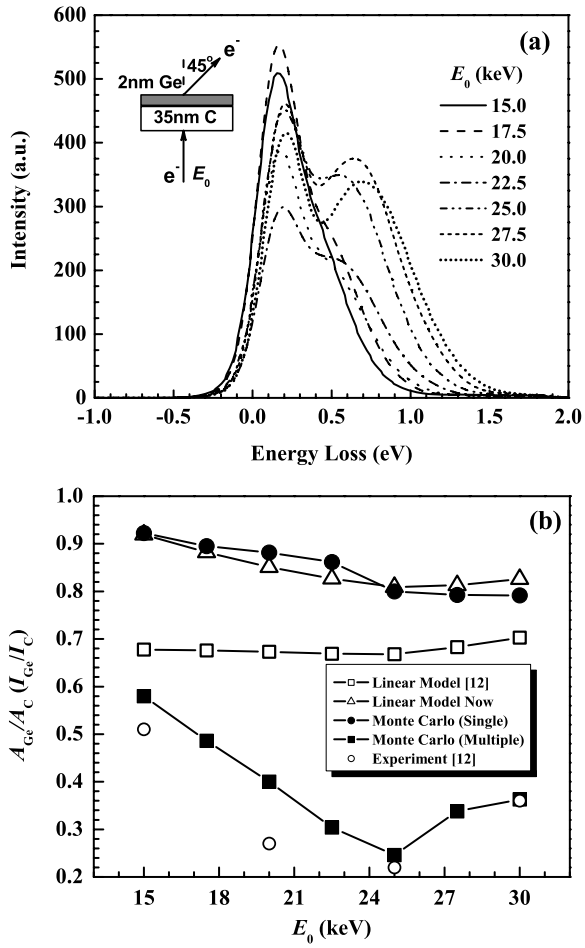

Figure 5. The incident energy dependence of the calculated (a) intensity profile and (b) intensity ratio, A_{Ge}/A_C, of the quasi-elastic peak of electrons normally incident on a Ge(2 nm)/C(35 nm) sample with the Ge layer on the exit side in the transmission mode. In (b) the comparison is also made with the Monte Carlo simulation of single scattering, available experimental data, the linear model with λ_{in} and the modified linear model with λ_{tr}.

the energy dependence of the spectra intensity. Although the elastic scattering cross section decreases rapidly with increasing energy so as to reduce elastic scattering signals, the IMFP increases simultaneously. This behavior of inelastic scattering allows more signal electrons to be emitted from the sample. Therefore, there has been no obvious primary energy tendency of spectra intensity found. However, on lowering the primary electron energy, the separation of the Ge and C peaks becomes small; at 15 keV it is even indistinguishable for the two peaks. Therefore, at lower primary energies the peak decomposition becomes more questionable, causing larger fitting error. Figure 5(b) demonstrates the relation of the intensity ratio A_{Ge}/A_C to the primary energy. It can be seen that with increasing primary energy (15–30 keV), the ratio decreases firstly and then increases; the minimum is at about 25 keV. The simulation indicates that this minimum is mostly resulting from multiple-scattering effects. The present calculation agrees with the experimental results very well, and greatly improves the previous quantitative results from a simple analysis [12]. It is worth mentioning that the choice of the parameters, $\bar{E}_k$ and k_0, does not affect the estimation of the intensity area under the curve. The correct intensity ratio calculation is largely due to the fair modeling of the electron

elastic and inelastic scattering cross section and the description of electron transportation.

The experimental fact has shown that the spectral profile depends strongly on the sample rotation geometry and on the reflection/transmission mode. In figure 6 both the experiment and calculation are performed at the condition of fixed value of scattering angle, 45°, between the incident beam and the detection direction, while the sample plane is tilted so that the incident angle and detection angle change simultaneously. The sample studied is a C(35 nm)/Ge(2 nm) film. Figures 6(a) and (b) are for the case where the electron incidence is on the C film surface, and figures 6(c) and (d) are for electron incidence on the Ge film surface. At normal incidence of electrons, the detection is in the transmission mode; by increasing the incident angle to exceed 45° the detection mode is changed to the reflection one.

Figures 6(a) and (c) thus illustrate the variation of the intensity profile with the changing of the incident angle. It can be seen that the calculated spectra profile of the elastic peak is altered dramatically with the sample tilting from transmission mode to reflection mode; the variation tendency of the intensity profile is quite similar to the experimental one. To be more quantitative, figures 6(b) and (d) plot the incident angle dependence of the intensity ratio $A_{\mathrm{Ge}}/A_{\mathrm{C}}$. In figure 6(b), for the incident angles smaller than 45°, an electron beam penetrates the sample film. Thus, both C and Ge signals are present; the Ge signal intensity will increase with the sample tilt up to 45° of the incident angle, at which the detection is at the glancing condition so the electrons should pass through quite a long distance before exiting from the Ge film surface. Therefore, the absolute intensity of the quasi-elastic peak will be lowered due to increasing of intensities of competitive scattering processes, i.e. events of multiple elastic and inelastic scattering. But the intensity ratio $A_{\mathrm{Ge}}/A_{\mathrm{C}}$ becomes very large as a detector selects more signal components from those scattering events due to electron collisions with the exit side atoms. For the incident angle larger than 45°, the detection is in the reflection mode and the backscattered electron signals from the Ge layer underneath drop suddenly while the signals from top C surface increase. This variation tendency is consistent with the experimental observation. In contrast, in figure 6(d), for the incident angle smaller than 45° the detector faces the C surfaces. Then, the absolute intensities of the quasi-elastic peak drop with increasing incident angle while more signals are due to C atoms in the exit side. In the reflection mode for the incident angles larger than 45°, the C signals are greatly reduced. However, a large deviation from the experimental data is found at 67.5°. It is noticed that the small value of the area for the weak C peak, in the denominator of intensity ratio, may induce a large estimation error.

In the above discussion we have not mentioned in detail the angular dependence of elastic scattering cross section. Actually, the differential cross section is atomic number dependent and the minor difference between two elements should also affect the calculated result for the angular dependence of the intensity ratio. We have neglected the surface excitation effect [34] in this simulation. These surface excitations are expected to influence the calculated

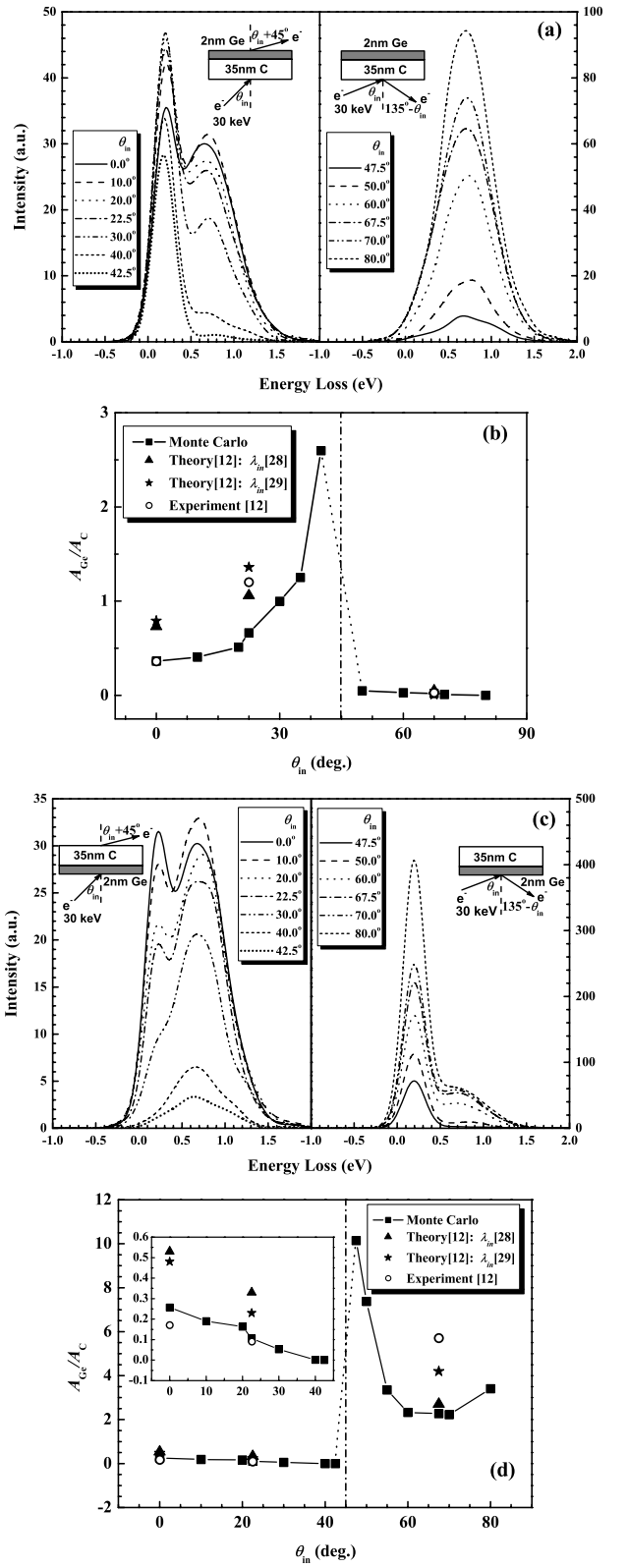

Figure 6. The incident angle dependence of ((a) and (c)) the intensity profile and ((b) and (d)) the intensity ratio, $A_{\mathrm{Ge}}/A_{\mathrm{C}}$, of the quasi-elastic peak of 30 keV electrons incident on a Ge(2 nm)/C(35 nm) sample. The detection geometry can be changed from the transmission mode (left in (a) and (c)) to the reflection mode (right in (a) and (c)) with the variation of the incident angle while the angle between the incident beam and detection direction is fixed at 45°. In (b) and (d) the comparison is also made with the available experimental data and simple theoretical analysis results.

intensity of the elastic peak through the strengthening of the competitive inelastic scattering probabilities [35, 36]; the surface excitation effect becomes important at glancing incidence/detection condition, but should be negligible for electrons of such high energy as 30 keV. The contribution of the surface excitations in the calculation has been further estimated by comparing the calculated high energy electron energy loss spectra (HEELS) without considering the surface excitation effect for the experimental ones [37]. For 40 keV electrons reflected from an aluminum surface a probability of just a few per cent for the surface excitations has been found. While aluminum is a nearly free electron metal with a prominent surface plasmon excitation, in contrast the influence of the surface excitations in C and Ge considered here would be negligible at such high energies.

As can be seen in all of the cases mentioned above, the present Monte Carlo simulation describes experiments much better than the linear model. The most likely reason is that the effects of multiple elastic scattering cannot be neglected in practice. For an energy loss peak measured at a specific scattering angle θ, the single-scattering event is for $\mathbf{q} = \mathbf{q}(\theta = \theta_1)$ while the double scattering is for $\mathbf{q} = \mathbf{q}_1 + \mathbf{q}_2$ $(\theta \sim (\theta_1, \theta_2))$, where θ_i is the scattering angle in the ith event. In figure 7 the Monte Carlo simulation results reveal that the signals due to the events of multiple elastic scattering contribute dominantly to the peak intensity. Multiple elastic scattering affects thus the intensity ratio of the quasi-elastic peaks, between different elements. For example, on considering multiple-scattering effects the intensity of the C peak is increased much more than that of the Ge peak, reducing the peak ratio $A_{\mathrm{Ge}}/A_{\mathrm{C}}$ (figure 5(b)). The sample condition may contribute to the remaining minor difference in intensity ratio between the experiment and calculation.

Figure 7 also shows that the multiple scattering does not alter the peak shape. This is due to difference in energy shifts between the approaches (where the events of multiple elastic scattering are included and where only single-scattering events are considered) being much smaller than the Doppler broadening value. For example, the expected maximum energy difference between single-scattering and the special double-scattering case with $\theta_1 = \theta_2 = \theta/2$ at $\theta = 45°$ is about 0.14 eV for the C peak at 30 keV. But actually the simulation indicates that the most probable value for such a difference is only 0.02 eV. This is simply due to the fact that the dominant double-scattering events are combinations of one small-angle scattering event and one large-angle scattering event ($\theta_1 \approx 0, \theta_2 \approx \theta$ or $\theta_1 \approx \theta, \theta_2 \approx 0$) as the differential scattering cross section is peaked at small scattering angles at such high energies. Thus, the multiple-scattering events have nearly the same peak position as the single-scattering event and could not be experimentally discriminated.

From the above simulation result, it is suggested that the linear model for single scattering [12, 38] could be improved by replacing the electron IMFP λ_{in} with the transport mean free path λ_{tr}. This is based on the consideration of the attenuation by events of multiple elastic scattering, which also reduce the emission probability of the single-scattering signals in the linear model, in addition to the attenuation by inelastic

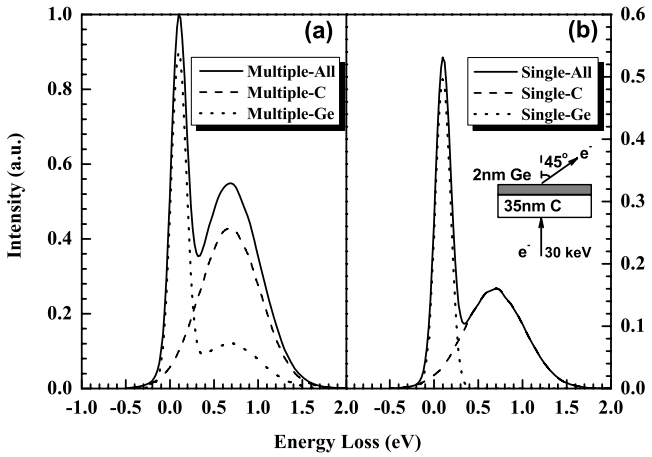

Figure 7. Monte Carlo simulation of quasi-elastic peaks but neglecting inelastic scattering background for a 30 keV electron beam incident normally on a Ge(2 nm)/C(35 nm) sample with a Ge layer at the exit side. Left: including multiple-scattering events ($n > 2$); right: considering only single-scattering events ($n = 1$). The solid line is the total intensity; the dashed and dotted curves represent, respectively, the contribution by the quasi-elastic scattering event lastly occurring before emission in the C layer and Ge layer.

scattering event. For $\lambda_{\mathrm{tr}}^{-1} = \lambda_{\mathrm{e}}^{-1} + \lambda_{\mathrm{in}}^{-1}$, where λ_{e} is the electron elastic mean free path, the attenuation of the signal is underestimated if only we are considering inelastic attenuation. As shown in figure 5(b), with such a modification the linear model presents an intensity ratio curve whose shape is quite similar to the Monte Carlo simulation and the experimental results.

Finally we discuss the parameter k_0 introduced for the correction of the position shift of the elastic peak spectra. The most probable value of E_{r} in equation (5),

$$\bar{E}_{\mathrm{r}} = \left[1 - \frac{k_0}{P}\frac{1}{\sin(\theta/2)}\right]\frac{q^2}{2M}, \tag{12}$$

is shifted to a smaller value as compared with E_{r0} in equation (2). The net correction $|\Delta E_{\mathrm{r}}| = |\bar{E}_{\mathrm{r}} - E_{\mathrm{r0}}| = \frac{k_0}{P}\frac{1}{\sin(\theta/2)}\frac{q^2}{2M}$ is proportional to the inverse of mass of the atom, and smaller for heavier elements as indicated by the experimental results. By assuming that k_0 is constant, about the incident electron energy, the relative correction value of the shift, $|\Delta E_{\mathrm{r}}|/E_{\mathrm{r0}} = k_0/[P\sin(\theta/2)]$, fits the experimental data reasonably well, at least in the high energy region, as shown by figure 8. Comparison of figures 8(a) and (b) indicates that k_0 is scattering angle dependent. A further theory is expected to improve this phenomenological analysis.

4. Conclusion

Quasi-elastic electron scattering from an overlayer/substrate system has been studied using a Monte Carlo simulation method. By introducing a preferential oriented momentum $\mathbf{k}_0$ for describing the anisotropic vibration of atoms, the recoil shift for the peak position of the quasi-elastic electron spectra can be well corrected. Monte Carlo simulations of intensity

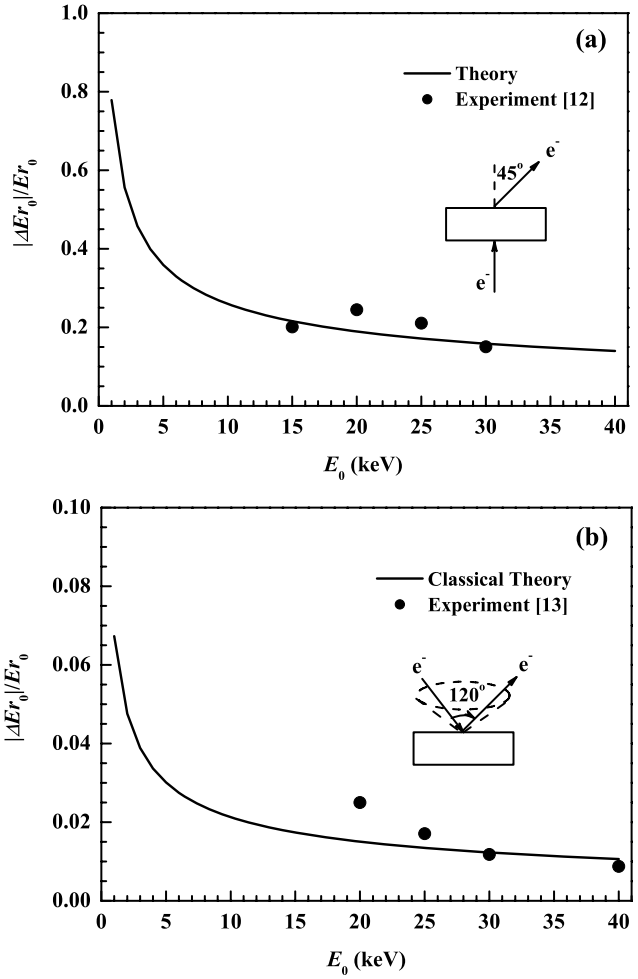

Figure 8. The dependence of the relative shift $|\Delta E_r|/E_{r0}$ of the quasi-elastic peak on the electron energy. The solid line is calculated using the equation $|\Delta E_r|/E_{r0} = k_0/[P\sin(\theta/2)]$, assuming that the parameter k_0 is independent of the electron energy. The solid symbol represents the experimental data. (a) $k_0 = 47.7$ nm^{-1}, $\theta = 45°$ [12]; (b) $k_0 = 9.58$ nm^{-1}, $\theta = 120°$ [13].

profiles of quasi-elastic peak spectra have been carried out for a Ge/C sample by varying the thickness of the layers, the incident electron energy and the detection mode. The simulation results are compared with the experimental measurements at the same conditions, enabling the discussion of the properties of the quasi-elastic electron scattering in detail: first, the intensity of the quasi-elastic electron spectra follows an exact linear relation with the thickness of the layers; second, the intensity of the quasi-elastic electron spectra has no simple relation with the incident electron energy as resulting from the complex elastic and inelastic scattering property; third, the relative intensity of the quasi-elastic electron spectra due to different atoms depends strongly on the incidence/detection angle and reflection/transmission mode. In most cases our Monte Carlo simulation describes very well the intensity profile and, particularly, the quantitative value of the intensity ratio. It is indicated that the multiple-scattering signals provide the dominant contribution to the intensity, while many of them are combinations of small-angle scatterings with one large-angle scattering. This simulation model is expected to handle samples like overlayer/substrate, alloy and compound, in the form of either multilayer film or bulk matrix, and the detection mode of either reflection or transmission.

Acknowledgments

This work was supported by the National Natural Science Foundation of China (Grant Nos 10574121, 10025420), '111 Project', Chinese Education Ministry and Chinese Academy of Sciences.

References

[1] Gergely G 2002 *Prog. Surf. Sci.* **71** 31
[2] Boersch H, Wolter R and Schoenebeck H 1967 *Z. Phys.* **199** 124
[3] Erickson N E and Powell C J 1989 *Phys. Rev.* B **40** 7284
[4] Laser D and Seah M P 1993 *Phys. Rev.* B **47** 9836
[5] Gergely G, Menyhard M, Benedek Z, Sulyok A, Kover L, Toth J, Varga D, Berenyi Z and Tokesi K 2001 *Vacuum* **61** 107
[6] Sulyok A, Gergely G, Menyhard M, Toth J, Varga D, Kover L, Berenyi Z, Lesiak B and Kosinski A 2001 *Vacuum* **63** 371
[7] Orosz G T, Gergely G, Menyhard M, Toth J, Varga D, Lesiak B and Jablonski A 2004 *Surf. Sci.* **566–568** 544
[8] Varga D, Tokesi K, Berenyi Z, Toth J and Kover L 2006 *Surf. Interface Anal.* **38** 544
[9] Went M R and Vos M 2007 *Appl. Phys. Lett.* **90** 072104
[10] Vos M 2002 *Phys. Rev.* A **65** 012703
[11] Vos M 2002 *Ultramicroscopy* **92** 143
[12] Went M R and Vos M 2006 *Surf. Sci.* **600** 2070
[13] Vos M and Went M R 2007 *Surf. Sci.* **601** 1536
[14] Varga D, Tokesi K, Berenyi Z, Toth J, Kover L, Gergely G and Sulyok A 2001 *Surf. Interface Anal.* **31** 1019
[15] Kwei C M, Li Y C and Tung C J 2004 *J. Phys. D: Appl. Phys.* **37** 1394
[16] Fujikawa T, Suzuki R and Kover L 2006 *J. Electon Spectrosc. Relat. Phenom.* **151** 170
[17] Ding Z J and Shimizu R 1996 *Scanning* **18** 92
[18] Li H M and Ding Z J 2005 *Scanning* **27** 254
[19] Ding Z J and Li H M 2005 *Surf. Interface Anal.* **37** 912
[20] Went M R and Vos M 2008 *Nucl. Instrum. Methods* B **266** 998
[21] Vos M and Went M R 2006 *Phys. Rev.* B **74** 205407
[22] Shimizu R and Ding Z J 1992 *Rep. Prog. Phys.* **55** 487
[23] Mott N F 1929 *Proc. R. Soc.* A **124** 425
[24] Bonham R A and Strand T G 1963 *J. Chem. Phys.* **39** 2204
[25] Yamazaki Y 1977 *PhD Thesis* Osaka University, unpublished
[26] Penn D R 1987 *Phys. Rev.* B **35** 482
[27] Tanuma S, Powell C J and Penn D R 1991 *Surf. Interface Anal.* **17** 911
[28] Tanuma S, Powell C J and Penn D R 1993 *Surf. Interface Anal.* **20** 77
[29] Tanuma S, Powell C J and Penn D R 2005 *Surf. Interface Anal.* **37** 1
[30] Ding Z J and Shimizu R 1989 *Surf. Sci.* **222** 313
[31] Mayers J, Burke T M and Newport R J 1994 *J. Phys.: Condens. Matter* **6** 641
[32] Williams M W and Arakawa E T 1972 *J. Appl. Phys.* **43** 3460
[33] Palik E D 1985 *Handbook of Optical Constants of Solids* (Orlando, FL: Academic)
[34] Ding Z J and Shimizu R 2000 *Phys. Rev.* B **61** 14128
[35] Tanuma S, Ichimura S and Goto K 2000 *Surf. Interface Anal.* **30** 212
[36] Jablonski A and Zemek J 2007 *Surf. Sci.* **601** 3409
[37] Li Y G, Ding Z J and Zhang Z M 2008 *Nucl. Instrum. Methods* B at press
[38] Jablonski A and Powell C J 2004 *Surf. Sci.* **551** 106